Synthesis and Crystal Structures of Four Cyanide-Bridged Coordination Polymers

Xiang He,[a] Can-Zhong Lu,*[a] Da-Qiang Yuan,[a] Shu-Mei Chen,[a] and Jiu-Tong Chen[a]

Keywords: Bridging ligands / Coordination polymers / Copper / Cyanides / Heterometallic complexes

The hydrothermal reaction of $Cu(NO_3)_2{\cdot}3H_2O$, $K_3Fe(CN)_6$, and 1,10-phenanthroline (1,10-phen) or 2,2′-bipyridine (2,2′-bpy) gives rise to the three one-dimensional helical-chain complexes $[Cu_2Fe(CN)_4(1,10\text{-phen})_3]_n{\cdot}0.5nH_2O$ (**1**), $[Cu_3(CN)_3(1,10\text{-phen})_3]_n$ (**2**), and $[Cu_3(CN)_3(2,2'\text{-bpy})_3]_n$ (**3**), and the two-dimensional layer complex $[Cu_3Fe(CN)_5(2,2'\text{-bpy})_2]_n$ (**4**). The structure of **1** contains a cyanide-bridged $Cu^I{\cdots}Fe^{II}{\cdots}Cu^I$ chain in which the two copper and one iron centers exhibit different coordination environments. The structures of **2** and **3** are both monometallic. Complex **4** is constructed alternately from fused 6- and 14-metal-membered nonplanar centrosymmetric rings that form a 2D layer architecture.

Introduction

The chemistry of spontaneously self-assembled supramolecular architectures based on transition metal complexes is currently an active and rapidly expanding research area. Transition metal cyanides have been studied for a long time because such compounds possess various interesting physical and chemical properties and have important applications in many fields, such as catalysis, molecular-based magnets, and zeolitic materials.[1–3] The cyanide group is a versatile ligand that can act as a monodentate ligand or as a bridging ligand adopting end-on (I) or end-to-end (II) modes to generate interesting complexes that may exhibit intriguing architectures and new topologies. As copper normally adopts three-, four-, five-, or sixfold coordination to form diverse geometric structures, much research has focused on the copper cyanide system from the viewpoint of structural engineering.[4,5] Helical structures have received special attention in the past decades as helicity is an essential element for bioactivity and also due to their potential applications in asymmetric catalysis and nonlinear optical materials.[6] To date, quite a few single- or double-helical chains have been generated,[7–9] with most helical polymers being obtained by using chiral ligands[10,11] or oligopyridines and other optically active ligands. In addition, the design and synthesis of novel coordination architectures can be controlled by varying the reaction conditions, including temperature,[12] metal-to-ligand ratio,[13] pH value,[14] solvents,[15] and counteranions.[16]

Generally, it is difficult to synthesise Fe^{II}-containing coordination polymers because the Fe^{II} ion is air-sensitive and hydrolyzes easily, and this might be the main reason why such Fe^{II} polymers are rare. In this article we report the syntheses and crystal structures of two Cu/Fe bimetallic cyanide-bridged coordination polymers – $[Cu_2Fe(CN)_4(1,10\text{-phen})_3]_n{\cdot}0.5nH_2O$ (**1**) and $[Cu_3Fe(CN)_5(2,2'\text{-bpy})_2]_n$ (**4**) – and two copper polymers – $[Cu_3(CN)_3(1,10\text{-phen})_3]_n$ (**2**) and $[Cu_3(CN)_3(2,2'\text{-bpy})_3]_n$ (**3**).

To the best of our knowledge, compound **1** is the first example of a one-dimensional helical chain structure that contains different metal atoms with quite different coordination environments, while compound **4** is the first example of a bimetallic neutral 2D lamella framework compound built up by cyanide-bridged 6- and 14-metal rings.

Results and Discussion

Hydrothermal methods are important in the synthesis of novel multidimensional open-framework materials as a change of reaction conditions for the preparation of these complexes can also have an effect on their structures, although it is difficult to control and predict the crystal structures under hydrothermal methods. It is known that the architectures of the products depend on many factors, such as temperature, the anions involved, the molar ratios of the precursors, the pH etc., and subtle adjustments of these parameters often result in the formation of quite different structures. For example, Forster and his co-workers have carried out systematic studies on the effect of temperature on the structures of the products.[12] Our syntheses under hydrothermal conditions provide four novel compounds with different structural frameworks (Scheme 1). Interestingly, we obtained two monometallic compounds and two

---

[a] The State Key Laboratory of Structural Chemistry, Fujian Institute of Research on the Structure of Matter, the Chinese Academy of Sciences,
Fuzhou, Fujian, 350002, China
Fax: +86-591-83714946
E-mail: czlu@ms.fjirsm.ac.cn

DOI: 10.1002/ejic.200400978

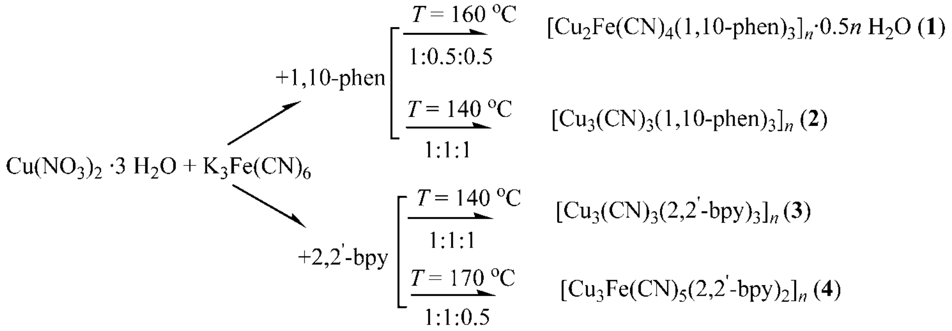

Scheme 1. Cyanide-bridged coordination polymers.

bimetallic materials from similar precursors. The reason for the different results obtained from these reactions is perhaps due to the temperature and the molar ratio of the precursors, although the details are not clear. From these processes $K_3Fe(CN)_6$ appears to be a promising precursor to obtain more new compounds.

The IR bands corresponding to CN stretching vibrations for compounds **1**–**4** appear in the range 2080–2116 cm^{-1}, which is typical for bridging cyanide groups. For **1**, two different absorptions at 2102 and 2080 cm^{-1} indicate the existence of two types of cyanide groups. The lower wavenumber band can be assigned to a terminal cyanide group, while the band at 2102 cm^{-1} is attributed to the stretching vibration of a linear bridging cyanide.

To study the stability of the polymers, thermogravimetric analysis (TGA) was performed for complexes **2**–**4**. These studies show that these complexes are stable up to 280 °C. The stabilities of these compounds make them potential candidates for practical applications.

Electron probe analyses revealed that there are two kinds of metals (copper and iron) in compounds **1** and **4**, the molar ratios of the two metals being 2:1 and 3:1, respectively, in agreement with the structural results. The magnetic susceptibilities of **1** and **4** are negative, which is typical of a diamagnetic behavior. This indicates that the iron atoms in these compounds are in the low-spin Fe^{II} ($S = 0$) state and the copper centers are in the Cu^{I} oxidation state.

$[Cu_2Fe(CN)_4(1,10\text{-phen})_3]_n \cdot 0.5n H_2O$ (1): A 1D Framework

The hydrothermal reaction of $Cu(NO_3)_2 \cdot 3H_2O$, $K_3Fe(CN)_6$, and 1,10-phen led to the formation of red crystals of compound **1**. X-ray analysis revealed that compound **1** has a one-dimension neutral helical-chain architecture. As the reaction was carried out under hydrothermal conditions, it is not surprising that the Cu^{II} and Fe^{III} ions have been reduced to Cu^{I} and Fe^{II} ions by cyanide or N-heterocyclic ligands, such as 1,10-phen or pyridine derivatives.[17–19] The cyanide in **1** is provided by the ferricyanide anions. A view of the metal coordination environment is presented in Figure 1. Two copper atoms have different co-

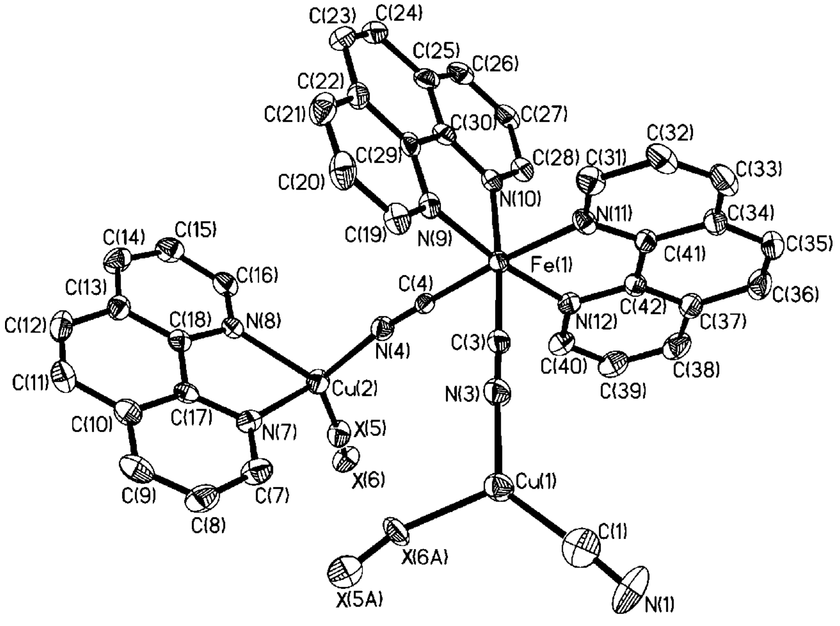

Figure 1. ORTEP representation of the polymeric structure of **1**, showing the coordination environments of the Cu and Fe centers (hydrogen atoms and solvent molecules have been omitted for clarity). Atoms from the disordered CN bridging groups are labeled as X.

ordination environments: the first Cu^I is coordinated by two cyanide [Cu–X = 1.904(7) Å and Cu–N = 1.969(5) Å] and two nitrogen atoms from 1,10-phen [Cu–N = 2.128(5) Å] and exhibits a distorted tetrahedral coordination environment, whereas the second Cu^I is coordinated by three nitrogen atoms from three cyanides [Cu–X = 1.932(9)–1.989(6) Å] and exhibits a distorted trigonal planar coordination environment. The heterocyclic 1,10-phen ligand is planar and the copper atom lies within this plane. The bond lengths and angles within the 1,10-phen group are in agreement with those reported for the free 1,10-phen molecule.[20] An intramolecular hydrogen bonding interaction C(28)–H(28A)···N(12) of about 3.098(8) Å is also present.

Each iron atom exhibits a distorted octahedral coordination environment and is coordinated by the carbon atoms from two cyanides and four nitrogen atoms from two bidentate 1,10-phen ligands. The bond lengths for the iron atom [Fe–C = 1.903(6)–1.928(5) Å and Fe–N = 1.973(5)–2.006(5) Å] and the corresponding angle subtended by the bidentate 1,10-phen ligand [N–Fe–N = 81.9(2)–82.2(2)°] agree well with those reported for the low-spin iron(II) complex $[Fe(1,10\text{-phen})_2(CN)_2]$.[21]

The intrachain distances Cu1···Fe1, Fe1···Cu2, and Cu1···Cu2 across cyanide bridges are 5.033(3), 4.985(2), and 4.939(2) Å, respectively. Each pair of adjacent metal atoms is bridged by cyanides to form a helical chain along the *b* axis with a pitch of 10.267(1) Å (Figure 2). The shortest interchain iron–iron, iron–copper, and copper–copper distances are 8.778(3) Å [Fe1···Fe1 (0.5 – *x*, 0.5 + *y*, 0.5 – *z*)], 6.574(1) Å [Cu1···Fe1 (1 – *x*, 1 – *y*, –*z*)], and 5.998(3) Å [Cu1···Cu1 (1 – *x*, 1 – *y*, –*z*)], respectively.

$[Cu_3(CN)_3(1,10\text{-phen})_3]_n$ (2): A 1D Framework

Compound **2** was obtained by varying the temperature and the composition of the reaction mixture used for the preparation of **1**. The X-ray diffraction study revealed that the copper atom is coordinated by two cyanide [Cu–X = 1.914(7)–1.919(9) Å] and two nitrogen atoms from 1,10-phen [Cu–N = 2.096(8)–2.138(8) Å] to give a distorted tetrahedral coordination environment (Figure 3). The cyanide ligands are linearly coordinated [C–N–Cu angles range from 173.3(7)° to 175.4(5)°] and bridge adjacent Cu^I atoms to form a one-dimensional helical chain running along the *c* axis with a long pitch of 24.485(10) Å (see a in Figure 4). The intrachain Cu···Cu distance across the cyanide bridges is 4.962 Å. This chain is decorated by 1,10-phen ligands above and below the helical chain. Figure 4 (see part b) shows that five copper atoms form two approximately equilateral triangles that have the same vertex, with the butterfly shape viewed down the *c* axis. The shortest interchain copper–copper distance is 7.751(3) Å [Cu1···Cu1 (0.5 + *x*, 1.5 – *y*, 1 – *z*)].

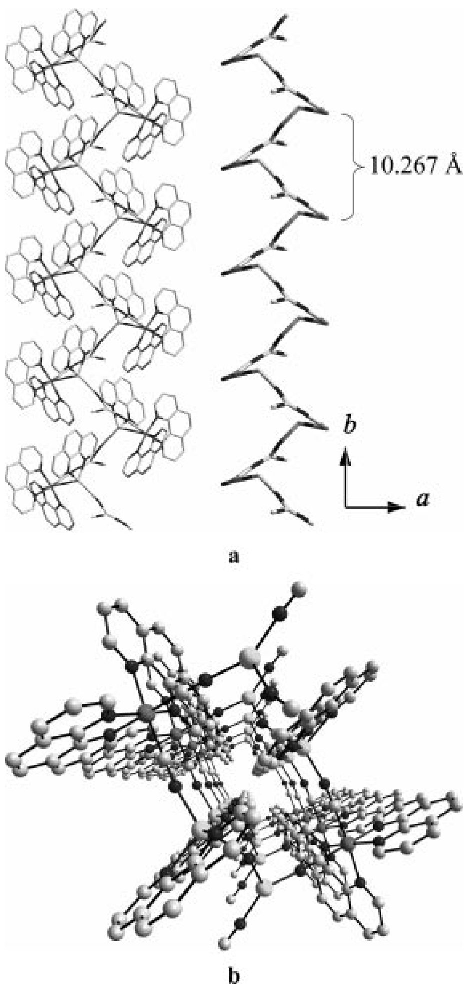

Figure 2. a) Schematic view of the helical chain of **1**. b) View along the helical axis.

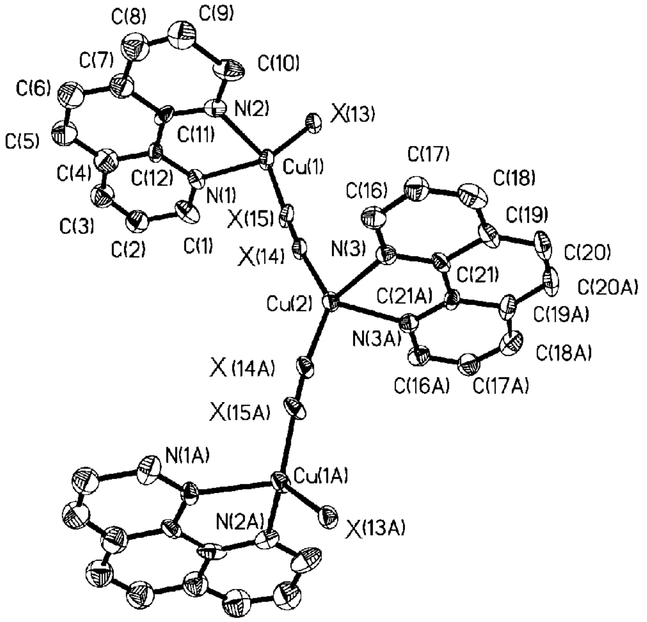

Figure 3. The coordination environments of the copper atoms in complex **2**.

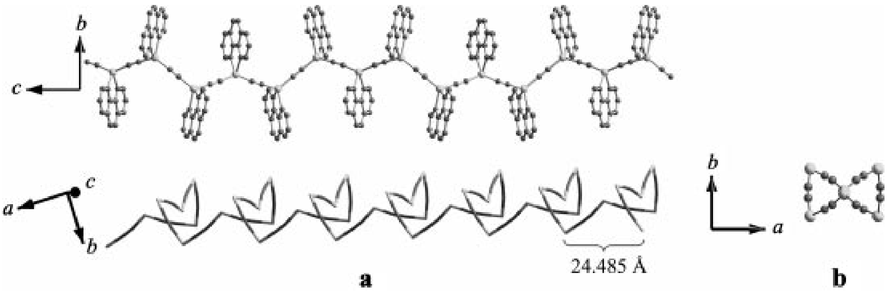

Figure 4. a) The 1D helical chain framework of **2**. b) View along the helical axis.

$[\mathrm{Cu(CN)(2,2'\text{-}bpy)}]_n$ (3): A 1D Framework

X-ray analysis revealed that the asymmetric unit of compound **3** consists of three neutral mononuclear molecules with copper center in a distorted tetrahedral environment. As shown in Figure 5, each copper atom is coordinated by two cyanides [Cu–X = 1.882(6) Å–1.930(5) Å] and two nitrogen atoms from 2,2′-bpy [Cu–N = 2.078(6) and 2.112(5) Å]. Every two adjacent $\mathrm{Cu^I}$ atoms are bridged by cyanides to form a chiral helical chain along the 3_2 screw axis with a long pitch of 12.898(1) Å (see a in Figure 6). The intrachain Cu···Cu distance across cyanide bridges is 4.973(1) Å. The helical chain with only a Cu–Cu backbone has a trigonal shape when viewed down the *c* axis, with each copper atom as the vertex of an approximately equilateral triangle. The angle subtended at the copper atom by two cyanide linkages is reduced to 126.8(2)° (b in Figure 6). This chain is also decorated by 2,2′-bpy ligands along both sides of the chain. The shortest interchain copper–copper distance is 7.371(1) Å [Cu1···Cu3 (1 – *x* + *y*, 1 – *x*, – 0.66667 + *z*)], which is slightly shorter than that for compound **2**.

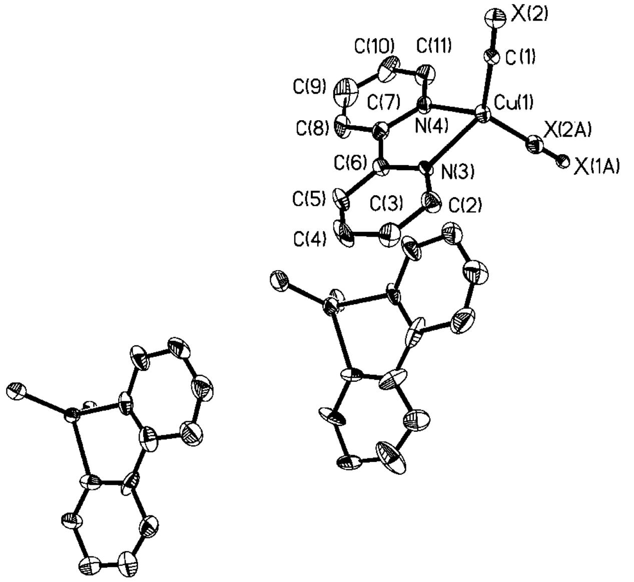

Figure 5. The coordination environments of the copper atoms in complex **3**.

$[\mathrm{Cu_3Fe(CN)_5(2,2'\text{-}bpy)_2}]_n$ (4): A 2D Network

Compound **4** was obtained by varying the temperature and the composition of the reaction mixture used for the preparation of **3**. The X-ray analysis revealed that the structure of **4** (Figure 7) consists of neutral corrugated sheets constructed alternately from fused 6- and 14-metal-membered nonplanar centrosymmetric rings, which are bridged by cyanide groups. Each 6-metal-ring contains two iron and four copper atoms, and the $\mathrm{Fe^{II}}$ atom is in a distorted octahedral environment containing four nitrogen atoms from two bipyridine ligands and two carbon atoms from two cyanide groups [Fe–N = 1.958(2)–1.986(3) Å; Fe–C = 1.909(3)–1.913(3) Å]. The values of the bond lengths in **4** for the iron atom are comparable to those found in compound **1** and other cyanide-bridged bimetallic complexes containing the $[\mathrm{Fe(bpy)_2(CN)_2}]$ building block.[22]

The two $\mathrm{Cu^I}$ atoms have two different coordination environments, with the first coordinated by three cyanide groups in a triangular geometry and the second coordinated by two cyanide groups in a linear geometry.

The Fe1···Cu1, Cu1···Cu4, Cu1···Cu2, and Cu2···Cu3 distances across cyanide bridges are 4.988(6), 4.870(7),

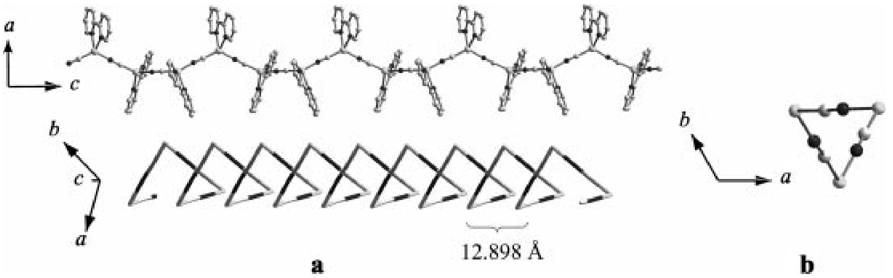

Figure 6. a) The 1D helical chain framework of **3**. b) View down the helical chain.

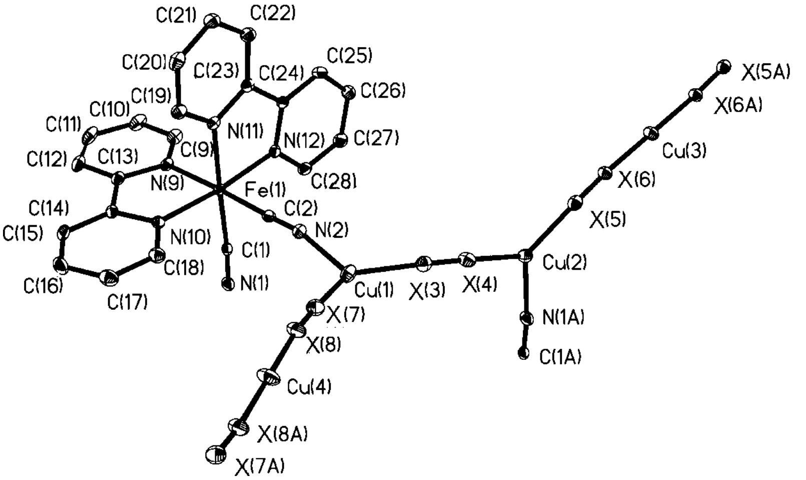

Figure 7. ORTEP representation of the polymeric structure of **4**, showing the coordination environments of the Cu and Fe atoms (hydrogen atoms have been omitted for clarity). Atoms from the disordered CN bridging groups are labeled as X.

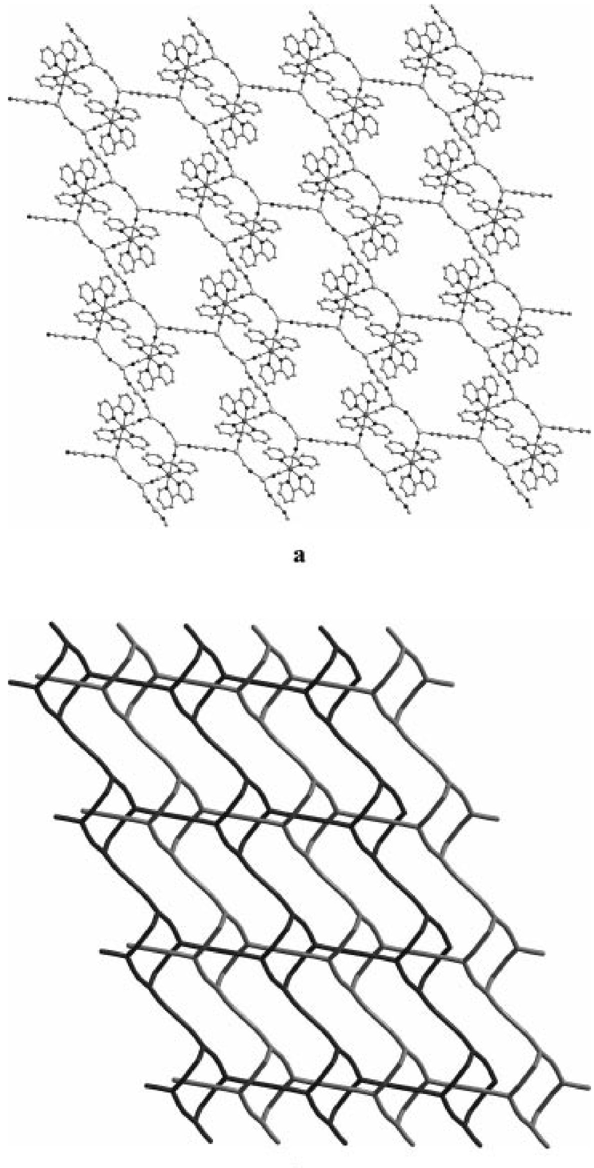

Figure 8. a) Perspective view of the 2D layer structure of **4**. b) Schematic representation of the interpenetrated 2D lamella framework.

4.901(13), and 4.840(16) Å, respectively. The structure consists of 2D layers, parallel to the *ac* plane, constructed by alternating 6- and 14-metal-membered centrosymmetric rings in which the metal centers are bridged by cyanide groups. The 6-metal rings adopt a chair conformation for the Cu···Fe···Cu···Cu···Fe···Cu unit. The size of these rings is about 8.9 × 8.0 Å^2. Four adjacent rings 6-metal rings add four two-coordinate copper atoms to form a larger 14-metal-membered ring {Fe-(Cu)$_6$-Fe-(Cu)$_6$} of approximately 13 × 22 Å^2. Each 14-metal-membered ring shares four sides with four adjacent 14-metal-membered rings and four sides with four adjacent 6-metal-membered rings; each 6-metal-membered ring shares all its edges with four 14-metal-membered rings to form a 2D framework. A view down the *b* axis shows that the actual crystal structure of compound **4** is a twofold interpenetrating 2D supramolecular framework (Figure 8). This is consistent with the fact that crystal structures with such large cavities are stabilized either by inclusion of suitable guests or by interpenetrating lattices.[23]

Intramolecular hydrogen-bonding interactions [C(9)–H(9A)···N(12) = 3.078(4) Å; C(19)–H(19A)···N(10) = 3.065(4) Å] also exist in **4**.

A method for preparing bimetallic compounds from hexacyanoferrate(III) under hydrothermal conditions has been reported previously.[24] Upon comparing the structure of **4** with the reported compound [Fe(bipy)$_2$(CN)$_4$Cu$_2$], it can be seen that the latter compound is constructed by alternately fused 6- and 10-metal-membered rings to form an ABAB pattern layer instead of the twofold interpenetrating structure found in compound **4**.

Conclusions

Three novel one-dimensional helical-chain coordination polymers and one two-dimensional layer complex have been obtained by hydrothermal synthesis. Under hydrothermal conditions, high-valence ions are reduced to low-valence ions by N-heterocyclic ligands or cyanide from ferricyanide anions. Furthermore, slow release of CN$^-$ might play an important role in the formation of these compounds. The successful isolation of these four compounds demonstrates that it is promising to use $K_3Fe(CN)_6$ as a precursor along with N-heterocyclic ligands, particularly derivatives of 2,2′-bpy and 1,10-phen, to construct novel coordination compounds under hydrothermal reaction conditions.

Experimental Section

General Remarks: All the syntheses were performed in poly(tetrafluoroethylene)-lined stainless steel autoclaves under autogenous pressure. Reagents were purchased commercially and were used without further purification. Elemental analyses of C and H were performed with an EA1110 CHNS-0 CE elemental analyzer. IR (KBr pellet) spectra were recorded on a Nicolet Magna 750FT-IR spectrometer. TGA analyses were carried out under nitrogen with a heating rate of 15 °C min^{-1} on a STA449C integration thermal analyzer. Electron probe analysis was performed with an EPM-810 EDAX9100 SHIMADZU electron probe microanalyzer. Variable-temperature (5–300K) magnetic susceptibility measurements were carried out on a Quantum Design MPMS-7 SQUID magnetometer at 5 T magnetic field using the SQUID method.

$[Cu_2Fe(CN)_4(1,10\text{-phen})_3]_n \cdot 0.5n\,H_2O$ (1): A mixture of $Cu(NO_3)_2 \cdot 3H_2O$ (0.02 g, 0.1 mmol), $K_3Fe(CN)_6$ (0.015 g, 0.05 mmol), and 1,10-phen (0.01 g, 0.05 mmol) in 20 mL of H_2O was stirred for 20 min at room temperature. The mixture was then transferred into a 30-mL, Teflon-lined stainless-steel vessel. The mixture was heated at 160 °C for two days under autogenous pressure. After the reaction mixture had slowly cooled down to room temperature, red prism-shaped crystals of **1** (0.02 g, 45% based on Cu) were collected. $C_{40}H_{25}Cu_2FeN_{10}O_{0.50}$ (863.65): calcd. C 57.42, H 3.01, Cu 15.19, N 16.74; found C 57.25, H 3.03, Cu 15.56, N 16.60. IR (KBr pellet): $\tilde{\nu}$ = 3552 m, 3421 m, 3049 m, 2102 vs, 2080 vs, 1628 m, 1421 s, 1342 m, 1205 m, 1142 m, 1051 m, 847 s, 777 w, 723 s, 633 w, 559 m cm^{-1}.

$[Cu_3(CN)_3(1,10\text{-phen})_3]_n$ (2): $Cu(NO_3)_2 \cdot 3H_2O$ (0.02 g, 0.1 mmol), $K_3Fe(CN)_6$ (0.03 g, 0.1 mmol), and 1,10-phen (0.02 g, 0.1 mmol) in 20 mL of H_2O were stirred for 20 min at room temperature. The mixture was then transferred into a 30-mL, Teflon-lined stainless-steel vessel. The mixture was heated at 140 °C for two days under autogenous pressure. After the reaction mixture had quickly cooled down to room temperature, red prism-shaped crystals were obtained (0.01 g, 45% based on Cu). $C_{39}H_{24}Cu_3N_9$ (809.29): calcd. C 57.88, H 2.99, Cu 23.56, N 15.58; found C 57.42, H 3.03, Cu 23.78, N 15.60. IR (KBr pellet): $\tilde{\nu}$ = 3415 m, 3057 m, 2107 vs, 2008 m, 1620 m, 1583 m, 1568 w, 1505 m, 1492 w, 1418 m, 1139 m, 841 s, 768 m, 727 s, 631 m cm^{-1}.

$[Cu_3(CN)_3(2,2'\text{-bpy})_3]_n$ (3): $Cu(NO_3)_2 \cdot 3H_2O$ (0.02 g, 0.1 mmol), $K_3Fe(CN)_6$ (0.03 g, 0.1 mmol), and 2,2′-bpy (0.016 g, 0.1 mmol) were added to 20 mL of H_2O. This mixture was stirred for 20 min at room temperature and was then transferred into a 30-mL, Teflon-lined stainless-steel vessel. The mixture was heated at 140 °C for two days under autogenous pressure. After the reaction mixture had slowly cooled down to room temperature, dark-red, prism-shaped crystals were obtained (0.01 g, 65% based on Cu). $C_{33}H_{24}Cu_3N_9$ (737.23): calcd. C 53.76, H 3.28, Cu 25.86, N 17.10; found C 54.02. H 3.36, Cu 25.53, N 17.53. IR (KBr pellet): $\tilde{\nu}$ = 3421 m, 3059 m, 2108 vs, 1593 m, 1470 m, 1439 s 1309 m, 1155 m, 1007 m, 764 s, 650 w, 417 w cm^{-1}.

$[Cu_3Fe(CN)_5(2,2'\text{-bpy})_2]_n$ (4): $Cu(NO_3)_2 \cdot 3H_2O$ (0.02 g, 0.1 mmol), $K_3Fe(CN)_6$ (0.03 g, 0.1 mmol), and 2,2′-bpy (0.008 g, 0.05 mmol) were added to 20 mL of H_2O. This mixture was stirred for 20 min at room temperature and was then transferred into a 30-mL, Teflon-lined stainless-steel vessel. The mixture was heated at 170 °C for two days under autogenous pressure. After the reaction mixture had slowly cooled down to room temperature, dark-red, prism-shaped crystals were obtained (0.006 g, 45% based on Cu). $C_{25}H_{16}Cu_3FeN_9$ (688.94): calcd. C 43.58, H 2.34, Cu 27.67, N 18.30; found C 43.56, H 2.64, Cu 27.89, N 18.49. IR (KBr pellet): $\tilde{\nu}$ = 3057 m, 2123 m, 2116 s, 2107 s, 1592 s, 1571 m, 1469 m, 1438 s, 1308 m, 1279 w, 1246 m, 1006 m, 792 s, 649 m cm^{-1}.

X-ray Crystallographic Study: Suitable single crystals of compounds with dimensions 0.34 × 0.32 × 0.30 mm (**1**), 0.30 × 0.20 × 0.20 mm (**2**), 0.50 × 0.18 × 0.10 mm (**3**), and 0.30 × 0.25 × 0.10 mm (**4**) were carefully selected and glued to thin glass fibers with epoxy resin. Crystal structure measurements for

Table 1. Crystal and structure-refinement data for compounds **1**–**4**.

Compound	**1**	**2**	**3**	**4**
Formula	$C_{40}H_{25}Cu_2FeN_{10}O_{0.5}$	$C_{39}H_{24}Cu_3N_9$	$C_{33}H_{24}Cu_3N_9$	$C_{25}H_{16}Cu_3FeN_9$
Mol. mass	863.65	809.29	737.23	688.94
Crystal system	monoclinic	orthorhombic	trigonal	triclinic
Space group	$P2_1/n$	$C222_1$	$P3_2$	$P\bar{1}$
a [Å]	13.1160(2)	8.515(4)	14.4307(8)	8.345(3)
b [Å]	10.2671(2)	16.616(9)	14.4307(8)	10.653(4)
c [Å]	25.7648(2)	24.485(10)	12.8975(11)	14.929(6)
α [°]				99.357(4)
β [°]	96.4740(10)			102.672(4)
γ [°]				93.668(4)
V [Å^3]	3447.45(9)	3464(3)	2326.0(3)	1270.8(8)
Z	4	4	3	2
D_c [g cm^{-3}]	1.612	1.552	1.579	1.800
$F(000)$	1692	1632	1116	684
μ [mm^{-1}]	1.687	1.868	2.078	3.070
GOF	1.048	1.104	1.040	1.072
R_1, wR_2 [$I > 2\sigma(I)$][a]	0.0616, 0.1279	0.0702, 0.1954	0.0552, 0.1465	0.0364, 0.0742
R_1, wR_2 (all data)[a]	0.0851, 0.1449	0.0791, 0.2027	0.0618, 0.1529	0.0504, 0.0821

[a] $R_1 = \Sigma(|F_o| - |F_c|)/\Sigma|F_o|$; $wR_2 = [\Sigma w(F_o^2 - F_c^2)^2/\Sigma w(F_o^2)^2]^{0.5}$.

Table 2. Selected bond lengths [Å] and angles [°] for compounds **1**–**4**.[a]

		Compound **1**			
Fe(1)–C(3)	1.903(6)	C(3)–Fe(1)–C(4)	88.9(2)	N(9)–Fe(1)–N(11)	93.5(2)
Fe(1)–C(4)	1.928(5)	C(3)–Fe(1)–N(12)	91.8(2)	N(10)–Fe(1)–N(11)	92.30(18)
Fe(1)–N(12)	1.973(5)	C(4)–Fe(1)–N(12)	93.8(2)	C(1)–Cu(1)–N(3)	132.3(3)
Fe(1)–N(9)	1.981(5)	C(3)–Fe(1)–N(9)	94.0(2)	C(1)–Cu(1)–X(6)^{I}	118.2(3)
Fe(1)–N(10)	2.000(5)	C(4)–Fe(1)–N(9)	90.6(2)	N(3)–Cu(1)–X(6)^{I}	109.3(2)
Fe(1)–N(11)	2.006(5)	N(12)–Fe(1)–N(9)	172.8(2)	X(5)–Cu(2)–N(4)	124.8(2)
Cu(1)–C(1)	1.878(8)	C(3)–Fe(1)–N(10)	175.7(2)	X(5)–Cu(2)–N(8)	110.2(2)
Cu(1)–N(3)	1.941(6)	C(4)–Fe(1)–N(10)	89.6(2)	N(4)–Cu(2)–N(8)	111.27(19)
Cu(1)–X(6)^{I}	1.985(6)	N(12)–Fe(1)–N(10)	92.39(19)	X(5)–Cu(2)–N(7)	118.0(2)
Cu(2)–X(5)	1.904(7)	N(9)–Fe(1)–N(10)	81.9(2)	N(4)–Cu(2)–N(7)	104.7(2)
Cu(2)–N(4)	1.969(5)	C(3)–Fe(1)–N(11)	89.5(2)	N(8)–Cu(2)–N(7)	78.40(19)
Cu(2)–N(8)	2.128(5)	C(4)–Fe(1)–N(11)	175.7(2)	C(3)–N(3)–Cu(1)	175.0(6)
Cu(2)–N(7)	2.128(5)	N(12)–Fe(1)–N(11)	82.2(2)	C(4)–N(4)–Cu(2)	171.5(5)
		Compound **2**			
Cu(1)–X(13)	1.915(7)	X(13)–Cu(1)–N(15)	123.5(3)	X(13)^{III}–X(13)–Cu(1)	175.4(5)
Cu(1)–X(15)	1.919(9)	X(13)–Cu(1)–N(2)	111.5(3)	X(14)^{II}–Cu(2)–X(14)	136.1(4)
Cu(1)–N(2)	2.096(8)	X(15)–Cu(1)–N(2)	109.1(3)	X(14)^{II}–Cu(2)–N(3)	109.5(3)
Cu(1)–N(1)	2.116(7)	X(13)–Cu(1)–N(1)	117.1(3)	X(14)–Cu(2)–N(3)	104.4(3)
Cu(2)–X(14)	1.914(9)	X(15)–Cu(1)–N(1)	107.8(3)	N(3)–Cu(2)–N(3)^{II}	77.3(4)
Cu(2)–N(3)	2.138(8)	N(2)–Cu(1)–N(1)	78.9(3)		
		Compound **3**			
Cu(1)–X(2)	1.886(6)	Cu(3)–N(7)	2.088(5)	X(13)–Cu(2)–N(5)	105.3(3)
Cu(1)–X(1)	1.930(5)	Cu(3)–N(8)	2.105(6)	N(6)–Cu(2)–N(5)	77.1(2)
Cu(1)–N(4)	2.103(5)	X(2)–Cu(1)–X(1)	127.0(2)	X(35)–Cu(3)–X(36)	126.9(2)
Cu(1)–N(3)	2.112(5)	X(2)–Cu(1)–N(4)	115.2(2)	X(35)–Cu(3)–N(7)	113.2(2)
Cu(2)–X(14)	1.893(9)	X(1)–Cu(1)–N(4)	101.6(2)	X(36)–Cu(3)–N(7)	105.3(2)
Cu(2)–X(13)	1.926(9)	X(2)–Cu(1)–N(3)	111.6(2)	X(35)–Cu(3)–N(8)	108.7(2)
Cu(2)–N(6)	2.078(6)	X(1)–Cu(1)–N(3)	112.7(2)	X(36)–Cu(3)–N(8)	114.9(2)
Cu(2)–N(5)	2.083(6)	N(4)–Cu(1)–N(3)	77.36(18)	N(7)–Cu(3)–N(8)	76.6(2)
Cu(3)–X(35)	1.882(6)	X(14)–Cu(2)–X(13)	125.9(3)	C(3)–N(3)–C(7)	119.5(5)
Cu(3)–X(36)	1.929(6)	X(14)–Cu(2)–N(6)	109.7(3)	C(3)–N(3)–Cu(1)	124.1(4)
		X(13)–Cu(2)–N(6)	113.4(3)	C(7)–N(3)–Cu(1)	116.2(4)
		X(14)–Cu(2)–N(5)	114.9(3)		
		Compound **4**			
Fe(1)–C(2)	1.909(3)	Cu(2)–N(1)^{IV}	1.957(3)	N(12)–Fe(1)–N(9)	94.66(10)
Fe(1)–C(1)	1.913(3)	Cu(3)–X(6)	1.829(3)	C(2)–Fe(1)–N(11)	89.53(11)
Fe(1)–N(10)	1.958(2)	Cu(4)–X(8)	1.821(3)	C(1)–Fe(1)–N(11)	177.31(11)
Fe(1)–N(12)	1.966(2)	C(2)–Fe(1)–C(1)	91.00(12)	N(10)–Fe(1)–N(11)	94.13(10)
Fe(1)–N(9)	1.979(2)	C(2)–Fe(1)–N(10)	94.47(11)	N(12)–Fe(1)–N(11)	81.25(10)
Fe(1)–N(11)	1.986(3)	C(1)–Fe(1)–N(10)	88.46(11)	N(9)–Fe(1)–N(11)	89.71(10)
Cu(1)–X(7)	1.895(3)	C(2)–Fe(1)–N(12)	89.30(11)	X(7)–Cu(1)–X(3)	127.49(13)
Cu(1)–X(3)	1.909(3)	C(1)–Fe(1)–N(12)	96.11(11)	X(7)–Cu(1)–N(2)	115.01(12)
Cu(1)–N(2)	1.949(3)	N(10)–Fe(1)–N(12)	174.03(10)	X(3)–Cu(1)–N(2)	115.72(12)
Cu(2)–X(5)	1.892(3)	C(2)–Fe(1)–N(9)	175.81(11)	X(5)–Cu(2)–X(4)	131.55(12)
Cu(2)–X(4)	1.910(3)	C(1)–Fe(1)–N(9)	89.96(11)	X(5)–Cu(2)–N(1)^{IV}	118.61(12)
		N(10)–Fe(1)–N(9)	81.47(10)	X(4)–Cu(2)–N(1)^{IV}	109.83(11)

[a] Symmetry transformations used to generate equivalent atoms: I: $-x + 3/2$, $y + 1/2$, $-z + 1/2$; II: $-x$, y, $-z + 1/2$; III: x, $-y + 2$, $-z + 1$; IV: $-x + 2$, $-y$, $-z + 1$.

compounds **1**–**4** were performed on a Rigaku Mercury CCD diffractometer with graphite-monochromated Mo-K_α radiation (λ = 0.71073 Å) at room temperature. A total of 6060, 3051, 5435, and 5718 unique reflections were collected in the $\omega/2\theta$ scan mode for **1**–**4**, respectively. The structures were solved by direct methods and refined on F^2 with the SHELXL97 program.[25] For all complexes the bridging cyanide group between two Cu^{I} atoms was disordered with respect to the C and N termini; this disorder was treated by performing test refinements with C and N atoms with partial occupancies. The disordered CN atoms positions are labeled in the tables and drawings as X. All non-hydrogen atoms were refined with anisotropic displacement parameters, and the hydrogen atoms were treated as riding atoms using the SHELX97 default parameters. For **1**, the hydrogen atoms of the water molecules were neither found nor calculated. For **2**, rigid refinement about the next six carbon atoms C4, C5, C6, C7, C11, and C12 was used to form a phenyl ring. The absolute structure parameters of compound **2** and **3** are 0.05(5) and 0.00, respectively. The crystal data and details of refinement for compounds are summarized in Table 1; selected bond lengths and angles are listed in Table 2.

CCDC-236440 (for **1**), -227060 (for **2**), -227061 (for **3**), and -243534 (for **4**) contain the supplementary crystallographic data for this paper. These data can be obtained free of charge from The Cambridge Crystallographic Data Centre via www.ccdc.cam.ac.uk/data_request/cif.

Acknowledgments

This work was supported by the 973 Program of MOST (001CB108906), the National Natural Science Foundation of China (90206040, 20425313, 20333070, and 20303021), the NSF of Fujian, and the Chinese Academy of Sciences.

---

[1] K. R. Dunbar, R. A. Heintz, *Prog. Inorg. Chem.* **1997**, *45*, 283–391.

[2] M. Verdaguer, A. Bleuzen, V. Marvaud, J. Vaissermann, M. Seuleiman, C. Desplanches, A. Sciuller, C. Train, R. Garde, G. Gelly, C. Lomenech, I. Rosenman, P. Veillet, C. Cartier, F. Villain, *Coord. Chem. Rev.* **1999**, *190*, 1023–1047.

[3] M. Ohba, H. Okawa, *Coord. Chem. Rev.* **2000**, *198*, 313–328.

[4] A. J. Blake, N. R. Brooks, N. R. Champness, M. Crew, L. R. Hanton, P. Hubberstey, S. Parsons, M. Schroder, *J. Chem. Soc., Dalton Trans.* **1999**, 2813–2817.

[5] S. R. Batten, A. R. Harris, P. Jensen, K. S. Murray, A. Ziebell, *J. Chem. Soc., Dalton Trans.* **2000**, 3829–3835.

[6] J.-M. Lehn, *Supramolecular Chemistry*, Wiley-VCH, Weinheim, **1995**.

[7] V. Soghomonian, Q. Chen, R. C. Haushalter, J. Zubieta, C. J. O'Connor, *Science* **1993**, *259*, 1596–1599.

[8] C. Piguet, G. Bernardinelli, G. Hopfgartner, *Chem. Rev.* **1997**, *97*, 2005–2062.

[9] F. G. Gelalcha, M. Schulz, R. Kluge, J. Sieler, *J. Chem. Soc., Dalton Trans.* **2002**, 2517–2521.

[10] D. Sun, R. Cao, Y.-Q. Sun, W-H. Bi, X. Li, M.-C. Hong, Y.-J. Zhao, *Eur. J. Inorg. Chem.* **2003**, 38–41.

[11] a) D. L. Reger, R. F. Semeniuc, M. D. Smith, *Eur. J. Inorg. Chem.* **2002**, 543–546; b) J. M. Rowland, M. M. Olmstead, P. K. Mascharak, *Inorg. Chem.* **2002**, *41*, 1545–1549; c) C. S. A. Fraser, D. J. Eisler, M. C. Jennings, R. J. Puddephatt, *Chem. Commun.* **2002**, 1224–1225.

[12] P. M. Forster, A. R. Burbank, C. Livage, G. Férey, A. K. Cheetham, *Chem. Commun.* **2004**, 368–369.

[13] A. J. Blake, N. R. Brooks, N. R. Champness, P. A. Cooke, A. M. Deveson, D. Fenske, P. Hubberstey, W.-S. Li, M. Schröder, *J. Chem. Soc., Dalton Trans.* **1999**, 2103–2110.

[14] X.-X. Hu, J.-Q. Xu, P. Cheng, X.-Y. Chen, X.-B. Cui, J.-F. Song, G.-D. Yang, T.-G. Wang, *Inorg. Chem.* **2004**, *43*, 2261–2266.

[15] M. A. Withersby, A. J. Blake, N. R. Champness, P. A. Cooke, P. Hubberstey, W.-S. Li, M. Schröder, *Inorg. Chem.* **1999**, *38*, 2259–2266.

[16] J. R. Black, N. R. Champness, W. Levason, G. Reid, *J. Chem. Soc., Chem. Commun.* **1995**, 1277–1278.

[17] a) J. Tao, Y. Zhang, M.-L. Tong, X.-M. Chen, T. Yuen, C.-L. Lin, X.-Y. Huang, J. Li, *Chem. Commun.* **2002**, 1342–1343; b) J. Tao, X. Yin, R.-B. Huang, L.-S. Zheng, *Inorg. Chem. Commun.* **2002**, *5*, 1000–1002.

[18] S. M.-F. Lo, S. S.-Y. Chui, L.-Y. Shek, Z. Lin, X. Zhang, G. Wen, I. D. Williams, *J. Am. Chem. Soc.* **2000**, *122*, 6293–6294.

[19] E. Colacio, R. Kivekäs, F. Lloret, M. Sunberg, J. S. Varela, M. Bardaji, A. Laguna, *Inorg. Chem.* **2002**, *41*, 5141–5149.

[20] S. Nishigaki, H. Yoshioka, K. Nakatsu, *Acta Crystallogr., Sect. B* **1978**, *34*, 875.

[21] S.-Z. Zhan, Q.-J. Meng, X.-Z. You, G.-W. Wang, P.-J. Zheng, *Polyhedron* **1996**, *15*, 2655–2658.

[22] H. Oshio, H. Onodera, O. Tamada, H. Mizutani, T. Hikichi, T. Ito, *Chem. Eur. J.* **2000**, *6*, 2523–2530.

[23] a) J.-C. Dai, X.-T. Wu, Z.-Y. Fu, S.-M. Hu, W.-X. D, C.-P. Cui, L.-M. Wu, H.-H. Zhang, R.-Q. Sun, *Chem. Commun.* **2002**, 12–13; b) R. E. Melendez, C. V. K. Sharma, M. J. Zaworotko, C. Bauer, R. D. Rogers, *Angew. Chem. Int. Ed. Engl.* **1996**, *35*, 2213–2215.

[24] E. Colacio, J. M. Dominguez-Vera, F. Lloret, J. M. M. Sanchez, R. Kivekäs, A. Rodriguez, R. Sillanpää, *Inorg. Chem.* **2003**, *42*, 4209–4214.

[25] G. M. Sheldrick *SHELXS97 Program for Solution of Crystal Structures*; University of Göttingen, Göttingen, Germany, **1997**.

Received: November 24, 2004